

Full-scale fire tests in the underwater tunnel section model with sidewall smoke extraction

Yaqiang Jiang^{1,#}, Tianhang Zhang^{2,#}, Shuai Liu³, Qinli He¹, Le Li¹, Xinyan Huang^{2,*}

¹*Sichuan Fire Research Institute, Ministry of Emergency Management, Chengdu, Sichuan, China*

²*Department of Building Environment and Energy Engineering, Hong Kong Polytechnic University, Hong Kong, China*

³*China Merchants Chongqing Communications Research & Design Institute Co., Ltd., Chongqing, China*

[#]*Joint first author, these authors contributed equally to this study*

^{*}*Corresponding to xy.huang@polyu.edu.hk (XH)*

Abstract

The Hong Kong–Zhuhai–Macau Bridge (HZMB) is a 55-km bridge-tunnel system, including a 6.7-km undersea tunnel that adopts the sidewall smoke extraction system. To evaluate the potential tunnel fire hazards, a 1:1 full-scale HZMB tunnel section model (16 m × 7.2 m × 150 m) was constructed, and eight full-scale tunnel fire tests were conducted with the sidewall smoke extraction. The temperature distribution and smoke movement under different vent arrangements and fire sizes (1.2 – 6.6 MW) were quantified. Results indicated that the fire HRR was mainly affected by the size of the liquid-fuel pool but insensitive to the arrangement of ventilation. The correlation between HRR and diesel pool-fire area can be fitted by a linear function of $HRR = 1.24 A_F - 0.87$ [MW]. The sidewall smoke extraction generated a tilted fire plume and non-uniform temperature distribution at the transverse direction, whereas the temperature decay still followed the exponential decay for the far fire field region. The decay factor increases with the increase of the HRR and increases when distributing the ventilation capability into two vent groups. A relatively slow smoke motion (0.8 – 1.2 m/s) and good smoke stratification were demonstrated in the tests, indicating a robust condition for safe evacuation. This research deepens the understanding of fire and smoke characteristics in tunnels with the sidewall extraction and highlights the importance of full-scale test data in the development of the smart tunnel-fire protection system.

Keywords: *Tunnel fire; Sidewall extraction; Temperature field; Smoke movement; Database*

Nomenclature

Symbols		Greeks	
A	area (m ²)	χ	combustion efficiency (-)
A_f	area of fuel (m ²)	ρ_a	the density of ambient air (kg/m ³)
AR	aspect ratio	θ	flame tilted angle (°)
c_p	specific heat capacity (J/kg · K)	η	heat remove efficiency
d	longitudinal distance (m)		
Fr	Froude number (-)		
g	gravity acceleration (m/s ²)	Superscripts	
h	flame height (m)	*	non-dimensional parameter
H	tunnel height (m)		
ΔH_c	heat of combustion (MJ/kg)	Subscripts	
k	decay factor (1/m)	a	ambient or air
l^*	non-dimensional back-layering length	b	back-layering or buoyancy
L	length (m)	C	critical
L_b	back-layering length (m)	eff	effective
\dot{m}_F	fuel burning rate (kg/s)	ref	reference point
\dot{V}	extraction rate (m ³ /s)	l	longitudinal
\dot{Q}_{sm}	heat remove rate of the vent (MW)	sm	smoke
T	temperature (°C)	t	transverse
ΔT^*	non-dimensional temperature rise (°C)	v	vent
u	smoke velocity (m/s)		
v	velocity (m/s)	Abbreviation	
W	tunnel width (m)	AI	artificial intelligence
x	longitudinal distance to the fire source (m)	GAN	generative Adversarial Net
y	transverse distance to the fire source (m)	HRR	heat release rate
z	vertical distance to the ground (m)	MLR	mass loss rate
		VG	vent group

1. Introduction

Currently, an increasing number of underwater tunnels are built to meet the rapid growth of traffic demand worldwide. For example, there is a 6.7-km long tunnel in the Hong Kong–Zhuhai–Macau Bridge (HZMB), which is the world’s longest immersed tunnel (Fig. 1a-b). The Channel Tunnel is a 50.5-km railway tunnel connecting the UK France beneath the English Channel at the Strait of Dover. However, fire incidences in underwater tunnels also bring serious safety risks to both occupants and tunnel structures. Five fire accidents have happened in the Channel Tunnel since 1994, causing significant economic losses (Fig. 1c). Compared with normal tunnels, underwater tunnels tend to be longer, deeper, and more enclosed, increasing the difficulty of fire protection, evacuation, and smoke extraction, so that the fire hazards are more deadly.

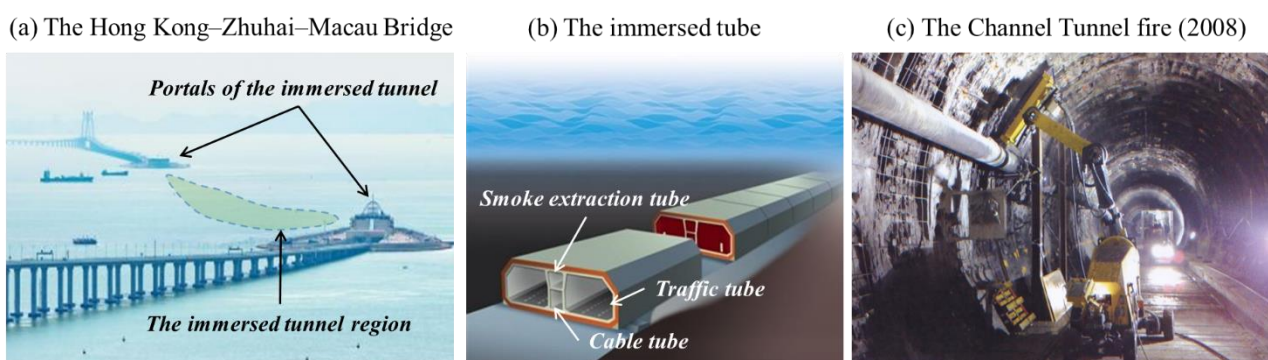


Fig. 1. (a) The Hong Kong–Zhuhai–Macau Bridge (HZMB), and (b) Diagram of the underwater tunnel, and (c) typical tunnel fire accidents.

The longitudinal ventilation system, fully transverse system, and semi-transverse system are most commonly found in road tunnels (Beard and Carvel 2012). Among the three types of ventilation systems, the longitudinal one was deemed to have the strongest smoke control ability, but it is not necessarily practicable for the underwater tunnel. Because the underwater tunnel typically has an extraordinary length and more restrictions in setting ventilation shafts. Therefore, the semi-transverse ventilation system was becoming more and more popular for underwater tunnels, requiring more fundamental research to improve fire safety and resilience. During the past decades, a large number of studies have been conducted on smoke control using the semi- and fully-transverse ventilation strategies with model experimental and numerical methods.

Vauquelin and Mégret (2002) firstly studied the smoke extraction performance within a 1:20 small-scale model tunnel and showed that the location of the vents had no significant influence on extraction efficiency. However, full-scale underground corridor fire tests conducted by Hu et al. (2006) showed that the extraction efficiency increased as the extraction vent was closer to the fire source. It is because the fire smoke temperature and buoyancy force decay when traveling along with the ceiling due to the heat loss, lowering the extraction performance away from the fire source. In fact, the conflict between the two tests indicated that the temperature field plays an important role in the smoke extraction

performance in semi-transverse ventilated tunnel fires, as well as the limitation of reduced-scale tests and the importance of full-scale tests.

Further theoretical and experimental work revealed that the smoke movement was dominated by the buoyance force and the inertia force for tunnel fires with the semi-transverse ventilation system, so that the smoke behaviors could be correlated with the Froude number and the Richardson number (Yang *et al.* 2010; Ingason and Li 2011; Chen *et al.* 2013). Effects of fire heat release rate (HRR), smoke flow state, number, and arrangement of vents on the smoke extraction efficiency were investigated numerically (Lin and Chuah 2008; Ji *et al.* 2012). The heat exhaust coefficient, defined as the ratio of the heat extracted rate to HRR (Xu *et al.* 2013), increased with the reduction of the vent number and size, and the increase of smoke temperature and vent extraction velocity (Yi *et al.*, 2015). For underwater tunnels, the extraction vents are typically designed on the sidewall (Fig. 1b) to fit the cross-section layout of the immersed tube (Lee *et al.* 2010), but related research is limited, especially in lack of full-scale fire tests.

Full-scale tunnel fire tests are the best representation of real fire scenarios, but they are also very limited due to the safety concern and the high cost. Valuable full-scale tunnel fire tests not only help validate small-scale tests and numerical results but also lay a foundation for future smart firefighting systems (Fu *et al.* 2021; Wu, Zhang, *et al.* 2021; Zhang, Wu, *et al.* 2021). Kurioka *et al.* (2003) studied the fire plume characteristics in the large-scale tunnel and proposed empirical equations to evaluate the flame tilt angle and maximum temperature rise. Hu *et al.* (2014, 2013, 2008, 2007a, 2006) investigated the fire smoke temperature profile and smoke back-layering phenomenon with different fire load and ventilation velocity by a series of full-scale tunnel fire tests. Ingason *et al.* (2005, 2006, 2015) conducted three groups of full-scale fire tests in Runehamar tunnel since 2005 to explore a wide spectrum of key tunnel-fire parameters. The effects of altitude on tunnel fire were studied by Yan *et al.* (2017) in Baimang Snow Mountain No. 1 Tunnel in Yunnan, China. Yang *et al.* (2020) studied the smoke movement characteristics in a full-scale sloped tunnel and found that the stack effect has a strong influence on sloped tunnel fire. Jiang and Ingason (2020) theoretically studied the transient behavior of flow development inside tunnel fires using mobile fans and validated using the test data from Kalldal tunnel fire tests. There are so far fewer full-scale tunnel fire tests with a sidewall extraction system to the best of the authors' knowledge. Xu *et al.* (2018, 2019) conducted a set of full-scale tunnel fire tests to investigate smoke spread and smoke layer height under longitudinal ventilation and proposed an optimal "uniform smoke extraction mode" to analyze the smoke discharge and energy-saving performance of sidewall smoke extraction. The spread of smoke layer was analysed as ideal 1-D flow, although the sidewall extraction causes a multi-dimensional smoke motion, and the smoke circulation within the cross-section is still unclear.

This work studies the smoke temperature distribution and smoke movement characteristics in a full-scale model of tunnel section (150 m long) with the sidewall extraction system, which was built with a 1:1 scale (cross-section) of the Hong Kong-Zhuhai-Macau Bridge underwater tunnel. The HRR, smoke

temperature, and movement are illustrated and compared with other ventilation systems from previous studies, and a database is established to support future AI-based smart firefighting systems.

2. Experimental Setup

A series of tests were conducted in a full-scale immersed tunnel that has a cross-section of 16 m (W) × 7.2 m (H) and a length of 150 m (Liu *et al.* 2016), as shown in Fig. 2a. The cross-section of this model tunnel is built with identical dimensions of the Hong Kong-Zhuhai-Macau Bridge immersed tunnel in China. The tunnel walls and ceilings are made of 0.7 m concrete materials. The tunnel represents a three-lane single traffic tube, and a smoke extraction duct is constructed adjacent to the tunnel structure.

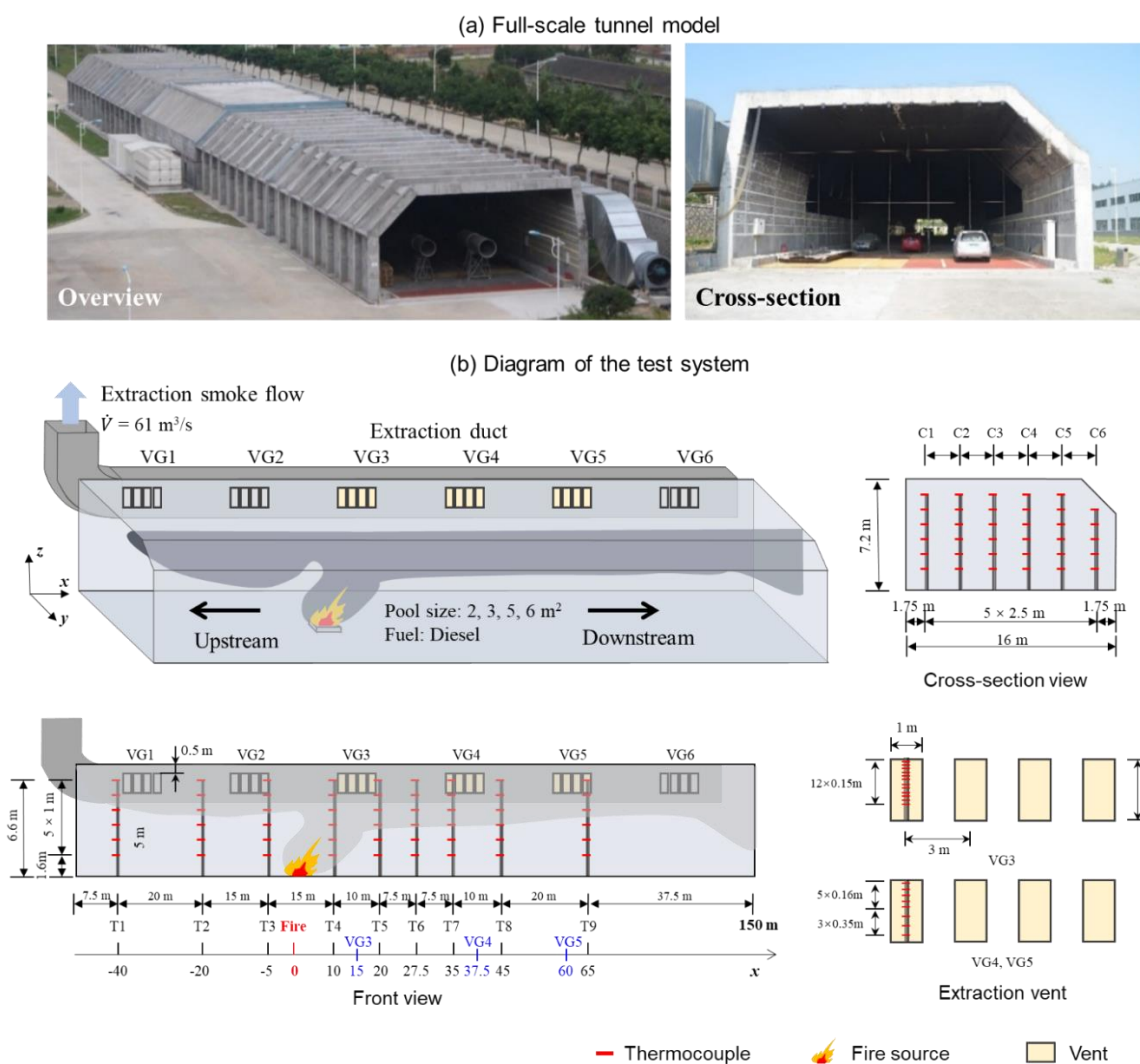


Fig. 2. (a) Full-scale tunnel model, and (b) diagram of the tunnel fire test system and layout of thermocouple trees.

The experimental setup is shown in Fig. 2b, where the coordinate follows \vec{x} (longitudinal), \vec{y} (transverse), and \vec{z} (vertical) throughout the paper. Six vent groups (VG) of smoke extraction (VG 1-6) are designed on one of the tunnel sidewalls, following the actual underwater tunnel design. Each vent

group consists of four individual openings with a dimension of 1 m × 2 m (i.e., vent area of 8 m² for each vent group) and a longitudinal length of 3 m. The distance between each adjacent vent group is 22.5 m, and the distance from the top of the vent to the tunnel ceiling is 0.5 m. Two ventilation fans with each extraction capacity of $\dot{V} = 61 \text{ m}^3/\text{s}$ were installed. During the fire tests, additional thermocouple trees were used to measure the gas temperatures at nine cross-sections (T1~T9) with a total of 315 measuring points. Previous studies (Ji et al., 2016; Zhang et al., 2021) indicate that the open boundaries will impact the smoke motion and temperature distribution at the near portal regions, and the impact length approximately equals the value of tunnel height (7.2 m for the present test). Therefore, the positions of thermocouple trees are designed to be as far from the tunnel portals as possible. The distances from T1, T9 to tunnel portals are 7.5 m and 37.5 m, respectively, which exceed the tunnel height value to avoid the boundary effect on the test data. Additional thermocouples were set in the opening to measure the temperature profile of the gas flow sucked into the vent.

Ideally, once a fire occurs, vehicles trapped upstream¹ of fire would stop, and drivers and passengers would evacuate by foot, vehicles downstream would continue moving in their original direction. Thus, it is of great importance to maintain a tenable condition in the upstream for fire evacuation and rescue. Following this principle, the operating vent groups were arranged in the downstream region from the fire source only. Eight full-scale tests were designed to investigate the influence of two kinds of factors on the smoke extraction performance of the sidewall transverse smoke control system. Major parameters considered in this research included the fire size and the arrangement of vent openings.

Table 1. Summary of the full-scale tunnel-fire experimental setup, where \surd means the vent group (VG) is open, where the fuel mass is the mass of diesel.

Test No.	Pool size (m ²)	Fuel mass (kg)	VG3 (x = 15 m)	VG4 (x = 40 m)	VG5 (x = 60 m)	T _a (°C)	V _a (m/s)	V _a / V _t (%)
1	2	15	\surd	\surd		17.2	< 0.1	<2.6
2	2	16	\surd		\surd	17.1	0.1	2.6
3	3	60	\surd			15	0.2	2.6
4	3	60	\surd	\surd		16.9	< 0.1	<2.6
5	3	60	\surd		\surd	15.9	< 0.1	<2.6
6	5	65	\surd			16.0	< 0.1	<1.3
7	5	100	\surd		\surd	15.6	< 0.1	<2.6
8	6	120	\surd			14.7	< 0.1	<1.3

Details of the experimental setup are given in Table 1. Fire size was limited during the test for safety consideration. The maximum pool size was 6 m², which is equivalent to the fire of small car. Diesel

¹ For conventional longitudinal ventilation system, the upstream is defined as the side that fire is closer to the exit.

was used as the fuel, and 2 kg of gasoline was adopted to ignite the pool fire in each test. During the test, the liquid pool was set on a fireproof board, and the real-time mass variety of the liquid pool fire was recorded with four weighing sensors, which is similar to that in the large-scale tunnel fire experiments carried out by (Yan *et al.* 2017). The mass data were recorded by a digital weight indicator (XK3190-AW1) with an interval of one second. The Heat Release Rate (HRR) was calculated by the Mass Loss Rate (MLR) measured in the test.

For the purpose of comparison, two operation modes of the vent groups were considered, i.e., operating only one vent group in the near field of fire and operating two vent groups both in the near-field and far-field. For scenarios with two vent groups, the distance between vents was also varied by selectively opening the 4th or the 5th group. The smoke extraction capacity of the fan was fixed to $\dot{V} = 61 \text{ m}^3/\text{s}$ (i.e., only one ventilation fan was used). Thus, the average transverse vent velocity (V_t) was 7.6 m/s for opening one vent group and 3.8 m/s for opening two vent groups. Before the experiments, the ambient temperature (T_a) and wind velocity (V_a) were measured. To minimize the impact of the natural ventilation on the smoke motion, the tests were conducted when the wind velocities were relatively small. It can be observed that for most tests, V_a was less than 0.1 m/s and the maximum value was 0.2 m/s in test 3. The ratio of the ambient wind velocity to average transverse vent velocity was lower than 3%, indicating that influence of the environmental wind was small. All data are available online https://github.com/PolyUFire/Tunnel_Fire_Database.

3. Results

A typical tunnel fire scenario with sidewall extraction is illustrated in Fig. 3. From a cross-section view, the hot fire smoke rises due to the buoyancy force. A ceiling jet happens when the smoke plume reaches the top boundary, and the direction of the mainstream converts to radial (Delichatsios 1981; Kunsch 2002).

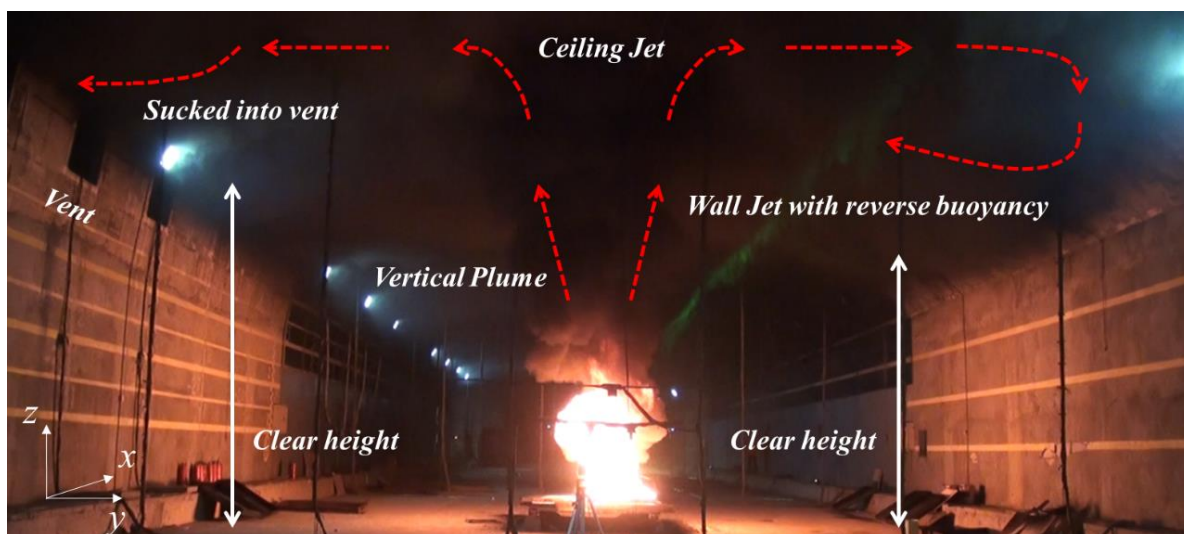


Fig. 3. A typical full-scale tunnel fire scenario with smoke transportation and ventilation (Test No. 1), where the direction is defined as longitudinal (\vec{x}), transverse (\vec{y}), and vertical (\vec{z}).

On the right side, a wall jet can be observed when the radially spread smoke reaches the sidewall. The wall jet flow has a direction that is reverse to the buoyancy, and then merges into the smoke layer. However, on the left side, the smoke was extracted into the vent directly. The wall jet process was broken and resulted in a thinner smoke layer and higher clear height near the vent, as indicated by arrows. The asymmetrical smoke flow characteristic caused by the extraction vent is the key difference between the sidewall extraction tunnel fire scenario and a longitudinally ventilated one. This section will explore and analyze the underlying characteristics of fire and smoke in the underwater tunnel with sidewall smoke extraction.

3.1. Heat release rate (HRR)

The tunnel is a typical semi-close space, so that the oxygen supply and heat feedback from the hot smoke and boundaries will significantly affect the combustion process of the pool fire. It is expected that the pool-fire characteristics in tunnels are different from the open space and influenced by the ventilation processes. The mass-loss rates (MLRs or the burning rate) of liquid fuel under various test conditions are plotted and compared in Fig. 4(a), which can be used further to derive the fire heat release rate (HRR). In general, based on the evolution of MLR, the fire development process can be typically divided into three stages, i.e., the growth stage, the stable stage, and the decay stage. Key parameters of the fire source and burning stage in each test are summarized in Table 2. In general, the growth stage is longer for a larger pool, where its duration increases from 72 s to about 137 s, as the pool area increases from 2 m² to 5 m². The MLR growth rate also increases as the pool-fire size increases, because of the greater heat feedback from the thicker and more turbulent flame.

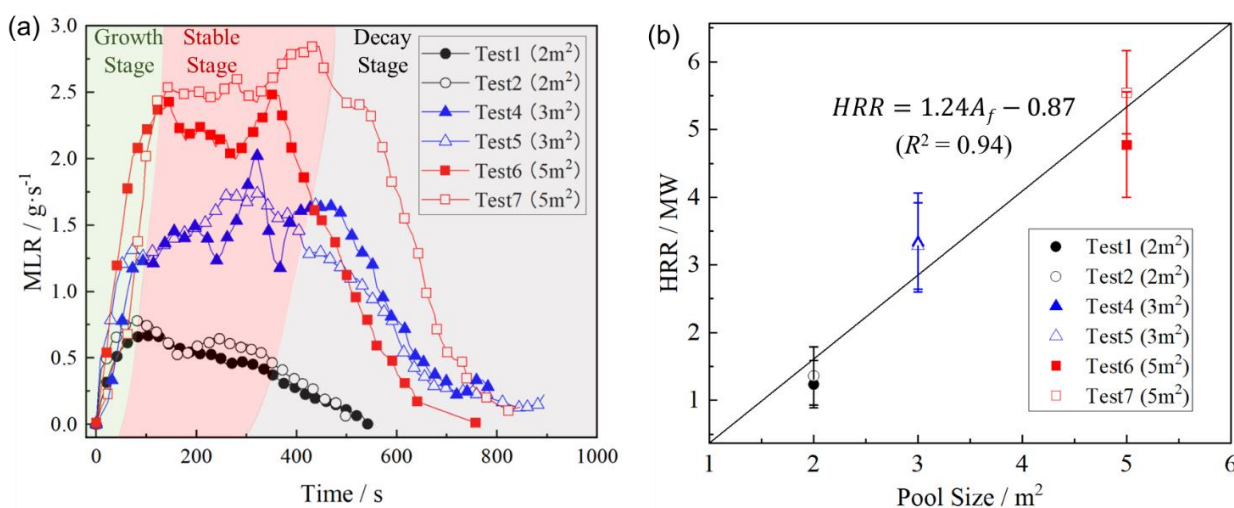


Fig. 4. (a) Fuel mass loss rate (MLR) against time, and (b) the average fire heat release rate (HRR) against the pool size for different tunnel-fire test cases. Technical issues of the weight scale occurred in Test Nos. 3 and 8, so their fuel mass data were not available

At the stable burning stage, the average variation of the MLR ranges from 10%-15%, and the stable duration increases with the amount of fuel, as shown in Fig. 4a. Note that there is large uncertainty in the tunnel fire test, so some approximations are needed to analyze the data. The stable stage was determined by most of the data points (more than 90%) located at the region with a fluctuation range of no more than $\pm 10\%$. Then, the time average MLRs at the stable stage is calculated, which increases significantly with the pool area, as shown in Table 2. Both tests 4 and 5 use two vents, except for different arrangement distances. However, no significant difference on the MLR curve is observed, and the HRR is almost the same (3.3 MW) for the two cases, indicating that VG4 is already too far from the fire source to affect the combustion process. These results provide key information for diesel pool fire development in tunnel fire scenarios with sidewall extractions.

The fire heat release rate (HRR) is one of the most important parameters in evaluating the fire intensity and hazards, and it typically can be calculated by the following equation (Zabetakis and Burgess 1961):

$$HRR = \chi \dot{m}_F \Delta H_c \quad (1)$$

where χ is the combustion efficiency, which is often set as 0.75 in typical tunnel fire scenarios (Hu, Huo, Wang, and Yang 2007; Hu, Huo, Wang, Li, *et al.* 2007); \dot{m}_F is the fuel MLR due to burning [$\text{kg}\cdot\text{s}^{-1}$]; ΔH_c is the heat of complete combustion [$\text{kJ}\cdot\text{kg}^{-1}$] which is $43 \text{ kJ}\cdot\text{g}^{-1}$ for diesel (Yan *et al.* 2017).

Table 2. Key burning-rate characteristics of the pool-fire source.

Test No.	1	2	4	5	6	7
Pool fire size (m^2)	2	2	3	3	5	5
Duration at the growth stage (s)	72	71	93	93	137	134
MLR growth rate ($\text{g}\cdot\text{s}^{-2}$)	0.53	0.59	1.11	1.10	1.08	1.28
Duration at the stable stage (s)	312	321	332	321	252	311
Average MLR at stable stage/ $\text{kg}\cdot\text{s}^{-1}$	0.038	0.042	0.103	0.102	0.148	0.172
HRR (MW)	1.2	1.4	3.3	3.3	4.8	5.5

Based on Eq. (1) and the average MLR in Table 2, the quasi-steady state HRRs of different pool sizes are calculated and plotted in Fig. 4b. It is well known that the burning rate of pool fire correlates with the pool size (Drysdale 2011). Thus, such a commonly used method is adopted here to fit the experimental data. The correlation between HRR and pool-fire area can be well fitted by a linear function of $HRR = 1.24 A_F - 0.87$ [MW]. Because of the large uncertainty in the measurement of mass loss rate, other parameters (wind velocity, fuel mass, etc.) were not further fitted to avoid over-interpretation. Meanwhile, since the selection of combustion efficiency (0.75) is an empirical value. Therefore, the correlation was only used as a reference value, and it will not be extended to different fire sizes and fuels.

3.2. Time evolution of temperature curve

Typical temperature evolutions of Test No. 1 at the vertical directions are summarized in Fig. 5a. Similar to the evolution of fuel MLR, three stages can be observed. The small pulsation in temperature is caused by the puffing flame and the turbulent smoke flow. The time average temperature is then adopted as the characteristic parameter in the following smoke dynamic analysis. At the vertical direction (\vec{z}), the temperature distribution indicates the smoke layer is in good stratification, i.e., a hot upper smoke layer lifted by the buoyancy force and a cold lower air layer. A clear gap can be observed between $z = 4.6$ m and $z = 5.6$ m, according to Fig. 5a, indicating that the height of the smoke layer is between 4.6 m to 5.6 m in the test.

At the longitudinal direction (Fig. 5b), smoke temperature decays in moving away from the fire source due to the convective heat loss to tunnel boundaries, the smoke radiation, and the cooling effect of the ventilation airflow (Ingason, Li, Lönnemark, *et al.* 2015; Zhao *et al.* 2018; Zhang, Wang, *et al.* 2021). Also, a sharp increase can be observed at the initial stage of the temperature curve, which also can indicate the arrival time of smoke to the location of the thermocouple and estimate the smoke movement characteristics (see more analysis in Section 3.5). The temperature curves of other test conditions have a similar trend, and the raw data have been uploaded to GitHub for further inquiry.

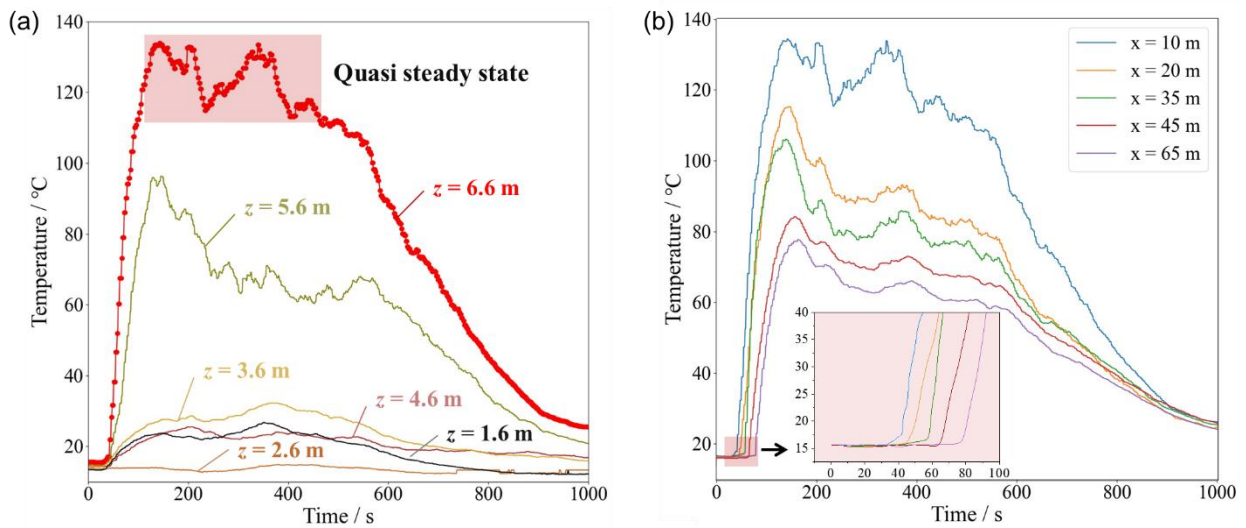


Fig. 5. Typical temperature distribution of Test No. 1, (a) in the vertical (\vec{z}) direction ($x = 10$ m, $y = -1.25$ m), and (b) in the longitudinal (\vec{x}) direction ($y = -1.25$ m, $z = 6.6$ m).

3.3. Transverse smoke temperature distribution

Non-dimensional parameters are widely used in tunnel fire research to connect the cross-scale experimental data (Wu and Bakar 2000; Li *et al.* 2010). For example, the non-dimensional temperature rise in the transverse direction (ΔT_t^*) and width (y^*) are defined as

$$\Delta T_t^* = \frac{\Delta T_t}{\Delta T_{max,t}} = \frac{T_t - T_a}{T_{max,t} - T_a} \quad (2a)$$

$$y^* = \frac{y}{W} \quad (2b)$$

where, T_t is the temperature at the same x and z positions, and y meters from the central line; T_a is the ambient temperature; $T_{max,t}$ is the global maximum temperature; and W is the tunnel width.

The effect of the sidewall vent on the non-dimensional temperature rise (ΔT^*) at $z = 6.6$ m (transverse direction) is plotted in Fig. 6. Generally, the temperature is higher near the sidewall vent. For example, at $x = -5$ m (upstream) and 10 m (downstream), there is a remarkable temperature difference ($\Delta T_t \approx 20\text{-}30$ °C) within the cross-section. On the other hand, as the distance from the fire source increases, the temperature difference within the cross-section decreases; for example, at $x = 45$ m, ΔT_t drops to 7 °C, which is comparable to the pre-fire temperature difference and the uncertain of the measuring system. This indicates that the current sidewall vent only affects the transverse temperature distribution at a relatively small region near the fire source.

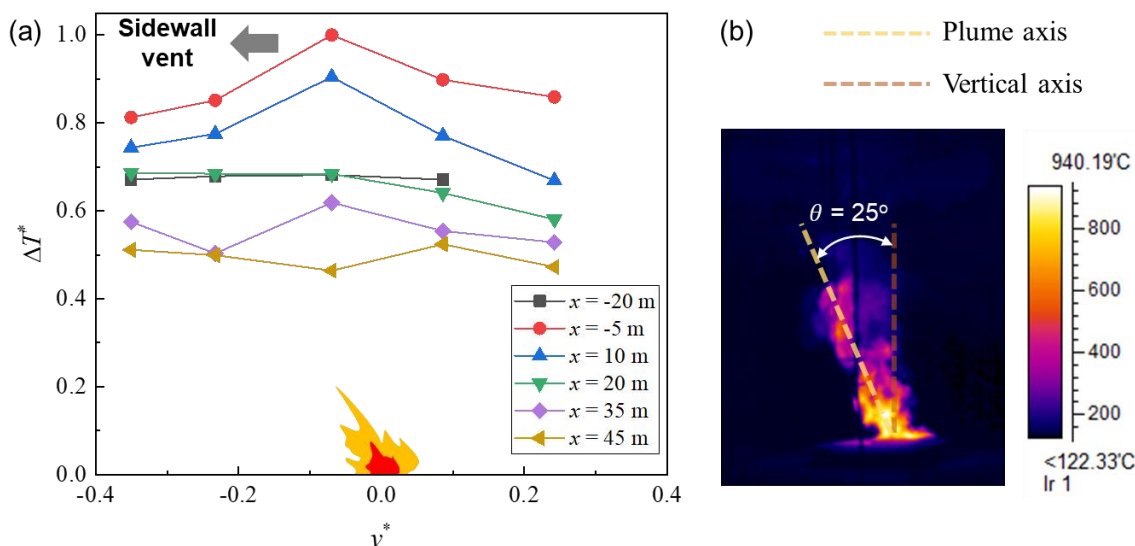


Fig. 6. (a) The non-dimensional smoke temperature rise in the transverse distribution (Test No. 1, $z = 6.6$ m), and (b) the IR image of the fire plume and tilted angle, where the value of temperature is only qualitative for reference.

Moreover, it is found that the fire plume tilts towards the sidewall vent, so that the current sidewall extraction is strong enough to affect the fire dynamics. The flame height of pool fire in Test No. 1 (2 m² and 1.2 MW) is 2.5 m. Thus, the buoyancy induced flow can be estimated as $v_b \approx \sqrt{gh} = 5$ m/s, where g is gravitational acceleration, valued as 9.8 m/s² and h is the flame height in m. Then, we can estimate the flame tilted angle (θ) under the sidewall extraction following the principle of Froude number (Fr)

$$Fr \approx \frac{v_t}{v_b} \approx \frac{\dot{Q}/A}{\sqrt{gh}} \quad (3a)$$

$$\tan\theta \approx \frac{v_b}{V_t} = \frac{1}{Fr} \quad (3b)$$

where the transverse vent velocity (V_t) is 3.8 m/s for opening two vent groups. Thus, the titled angle can be calculated as $\tan\theta \approx 3.8/5$ and $\theta = 35^\circ$. However, only a flame tilt angle of 25° was observed from the video in Fig. 6b, which indicated that the sidewall extraction effect was weaker than the calculation. Note that the non-uniform transverse distributed temperature is caused by the existence of the fire, and whether the flame tilting will increase or decrease the transverse temperature difference is still unclear.

To compare the non-uniformity in the smoke temperature's transverse distribution between different test conditions, the maximum transverse non-dimensional temperature difference (δT_t^*) is defined as:

$$\delta T_t^* = \Delta T_{max,t}^* - \Delta T_{min,t}^* \quad (4)$$

where $\Delta T_{max,t}^*$ and $\Delta T_{min,t}^*$ are the maximum and minimum non-dimensional temperature rises at the same y and z (see Fig. 6a). Note that δT_t^* is a non-dimensional parameter. Therefore, a large δT_t^* means a large non-uniformity of the transverse temperature distribution rather than a large absolute temperature difference.

Fig. 7a shows the effect of HRR and vent-group arrangement on δT_t^* in the longitudinal direction (\vec{x}), where $\delta T_t^* = 0.1$ is selected as the threshold to characterize the non-uniformity of the transverse temperature. As expected, the largest transverse temperature variation occurs near the fire region for all cases ($x = -10 \text{ m} \sim 20 \text{ m}$). As the fire HRR increases, the transverse temperature difference (δT_t^*) also becomes larger. For a small fire HRR (Test Nos. 1 and 2 with VG3 open at $x = 15 \text{ m}$), the transverse extraction ($v_t = 3.8 \text{ m/s}$) not only can tilt the flame and fire plume, but also maintain a large transverse temperature difference towards the opening vent group ($x > 0$).

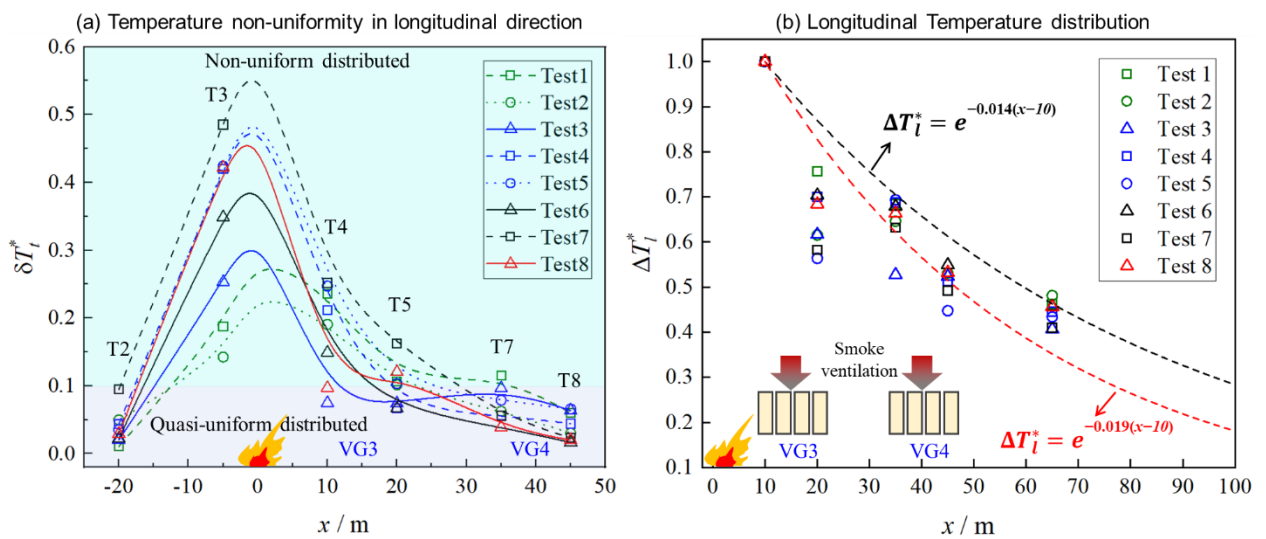


Fig. 7. Longitudinal distribution of (a) non-dimensional transverse temperature difference (δT_t^*), and (b) the non-dimensional temperature rise (ΔT_t^*).

Fundamentally, when there is an additional sidewall vent, the transverse extraction effect will lead the flame and plume tilted to the vent direction, as demonstrated in Fig. 6. It's believed that the smoke plume was driven by the vertical buoyancy and the transverse extraction, which was dominated by the sidewall vent air velocity. Owing to the fact that the temperature distribution was indeed the hot smoke distribution. Therefore, the transverse temperature profile is determined by the competition between the vertical buoyancy force and the transverse extraction.

For a small fire HRR, the flame height is smaller so that the buoyancy force is relatively weak, and the Froude number is larger. As seen from Eq. (3), the extraction tilts the fire plume towards the vent direction and results in a large temperature variation near the vent region. As the increase of fire HRR or flame height and the decrease of ventilation (v_t), the buoyant effect of the fire plume becomes stronger to lower the inclination angle. Thus, a larger transverse temperature non-uniformity appears upstream ($x < 0$, e.g., T3) due to the large HRR. In contrast, a smaller transverse temperature non-uniformity is found further downstream ($x \geq 20$ m, e.g., T5-T7) because of far away from the fire source. To further interpret test data and reveal the performance of sidewall extraction, more parameterized numerical and scaling analyses are needed in future studies.

3.4. Longitudinal smoke temperature distribution

During the smoke transport in the longitudinal direction (\vec{x}), the smoke-layer temperature decays due to the heat transfer to tunnel boundaries and radiation loss. Hu et al. (2008) experimentally studied the smoke longitudinal temperature decay by a set of full-scale tunnel fire tests and proposed an empirical correlation:

$$\Delta T_l^* = \frac{\Delta T_l}{\Delta T_{max,l}} = e^{-k(x-x_{ref})} \quad (5)$$

where ΔT_l is the temperature rise at the longitudinal direction, $\Delta T_{max,l}$ is the maximum temperature rise in the tunnel, x_{ref} is the longitudinal reference distance from the fire source, and k is the decay factor. The form of this equation has been well verified in multiple experiments and numerical simulations (Hu, Huo, Wang, Li, *et al.* 2007; Hu *et al.* 2008; Zhang, Wang, *et al.* 2021).

Fig. 7b shows the non-dimensional temperature distribution in the longitudinal direction in this work with sidewall smoke extraction, together with the fitting curves. Based on the analysis above and Fig. 7a, the transverse temperature distribution is relatively uniform beyond 10 m downstream from the fire source. Therefore, the exponential functions are adopted to fit the test data with thermocouple in T4 ($x = 10$ m, $y = -1.25$ m, $z = 6.6$ m) as the reference point, that is, $x_{ref} = 10$ m. The fitting results in Fig. 7b and Table 3 indicate that the longitudinal temperature distribution with sidewall smoke extraction can also be well fitted by the exponential function as Eq. (5) with a R^2 coefficient larger than 0.96.

Table 3. Fitting results of longitudinal non-dimensional temperature distribution and the decay factor (k).

Test No.	1	2	3	4	5	6	7	8
k (m^{-1})	0.015	0.014	0.019	0.016	0.017	0.015	0.018	0.015
R^2	0.98	0.98	0.97	0.98	0.96	0.99	0.99	0.99

According to the previous work, the smoke mass flow rate and fire heat release rate are two key parameters to affect the decay factor (Hu *et al.* 2008). By comparing the temperature decay factors for tests with the same ventilation arrangement and different HRRs (Test Nos. 2, 5, and 7), it is found that k increases as the HRR increases. This is because for a large fire, the smoke temperature is higher, and the heat loss of the smoke layer (heat conduction to tunnel boundaries and radiation) will increase accordingly. Therefore, the temperature decays faster, as observed in the table. Besides, when comparing the effect of the ventilation arrangement (Test Nos. 3, 4, and 5), k decreases when distributing the extraction capability into two vents. This is because the temperature will decay faster as the smoke mass flow rate decreases. In Test No. 3, more smoke will be extracted through VG3, causing the increase of the decay factor. Also, no significant difference can also be observed for Test Nos. 4 and 5, indicating the far-field vents have a relatively small influence on the smoke temperature field.

Moreover, most temperature measurements locate within the upper and lower fitting curves, except the temperature points of T5 ($x = 20$ m). Such a temperature drop is caused by the mass loss extracted by VG3 at $x = 15$ m between T4 and T5, which is a unique phenomenon for the sidewall extraction system. Moreover, as the longitudinal smoke mass flow rate is reduced by the sidewall vent, the longitudinal temperature will decay faster, resulting in a larger temperature decay factor (Zhang *et al.*, 2021). In short, despite the influence of the sidewall extraction system, the longitudinal temperature distribution has a relatively well one-dimensional characteristic at the far fire source field since δT_i^* distributed at around 0.1 for $x > 20$ m region and a temperature drop can be observed due to the mass loss when the smoke flow passed the vent. However, only a limited number of tests can be conducted in this work since the full-scale tests are both times and cost consuming. The temperature decay characteristics are only demonstrated by a few representative ventilation scenarios. More investigations (including both numerical research and scaled model tests) are needed to obtain comprehensive and quantitative conclusions in the future.

3.5. Smoke spread velocity

Smoke spread velocity is of great significance in tunnel fire as it provides essential information for evacuation and firefighting decisions. As mentioned in Section 3.2, the sharp increase of the temperature curve can be regarded as the arrival signal when hot smoke reaches the measuring point. The positions of smoke-layer leading edge with time at the longitudinal direction are shown in Fig. 8. It can be observed that the smoke spread distance appears to increase linearly with time, which indicates

the smoke spread velocity (i.e., the slope of the line) maintains a constant during the smoke's longitudinal movement (Yan *et al.* 2017).

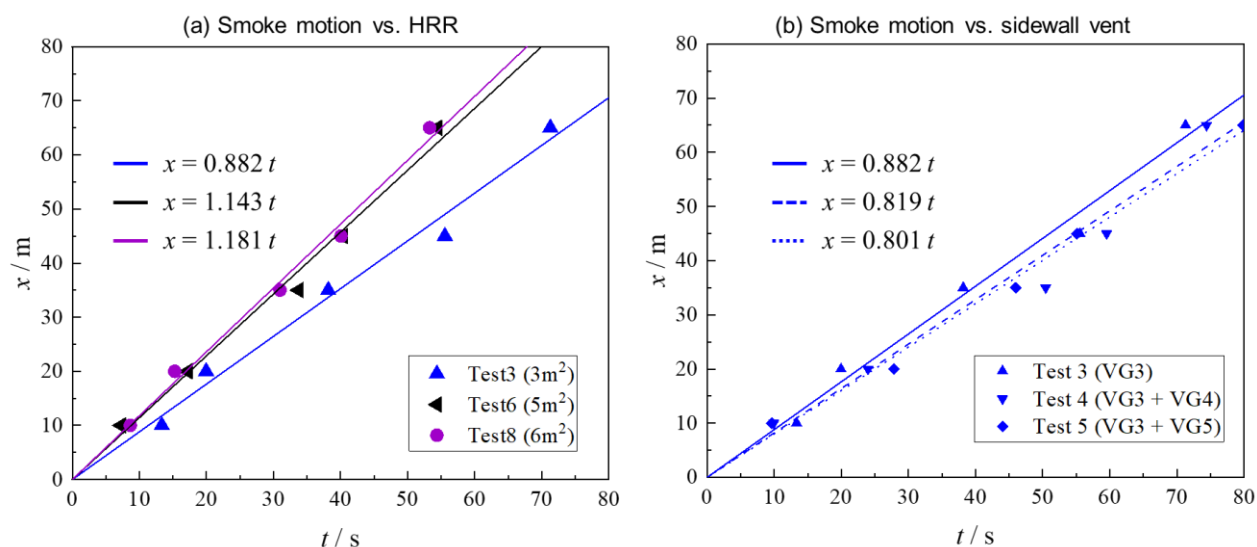


Fig. 8. Smoke longitudinal movement distances, (a) effect of fire HRR, and (b) effect of sidewall vent.

Also, as the fire HRR increases, the smoke movement gets faster. Fig. 8a shows that the smoke spread velocity (v_{sm}) increases from 0.88 m/s to 1.18 m/s when the pool size increases from 3 m² to 6 m², and the fire HRR increases from 1.2 MW to 6 MW. The movement of hot smoke layer is driven by the buoyancy, larger fire HRR normally releases hotter and more smoke (Liu *et al.* 2021). Thus, a stronger buoyant effect and more smoke mass flow rate led to a higher smoke spread velocity.

The effect of the vent arrangement on the smoke movement is compared between Test Nos. 3-5 in Fig. 8b with a similar fire HRR of 3-3.3 MW and the same extraction capability (61 m³/s). The smoke spread velocity is larger for one group vent case (Test No. 3) than those with two group vent cases (Test Nos. 4 and 5). In other words, with a given smoke extraction capability, more extraction vents can reduce the overall smoke movement velocity, which may bring more evacuation time. Moreover, smoke spread velocities in Test Nos. 4 and 5 are close to each other, with a relative difference of 2.2%. Thus, with the same vent number, the vent arrangement may only have a limited influence on the smoke spread velocity. In short, the smoke velocity in the current tests varies from 0.8 to 1.2 m/s, which is close to the full-scale tunnel fire tests with longitudinal ventilation system ($v_{sm} \approx 1$ m/s) (Hu *et al.* 2008). The comparison indicates that the smoke spread velocity is insensitive to the sidewall extraction system under the current extraction capacity.

4. Discussions

4.1. Smoke control performance

To study the smoke control performance of the sidewall extraction system, the observed smoke spread distances (L_{sm}) in this work are compared to the back-layering distance (L_b) in longitudinal

ventilation system with the same ventilation capacity (61 m³/s) in Table 4. The back-layering length was estimated by the empirical correlation (Li *et al.* 2010; Li and Ingason 2017) as:

$$l^* = 18.5 \ln(u_c^*/u^*) \quad (6)$$

$$u_c^* = 0.81(AR)^{-1/12} HRR^{*1/3} \quad (7)$$

$$HRR^* = \frac{HRR}{\rho_a c_p T_a g^{1/2} H_{eff}^{5/2}} \quad (8)$$

where $l^* = L_b/H$ is non-dimensional back-layering length; H is the tunnel height in m; H_{eff} is the effective tunnel height in m, which is defined as the distance from the top of fuel to the ceiling; $u_c^* = u_c/\sqrt{gH}$ is the non-dimensional critical velocity (or the characteristic Fr Number); u_c is the critical velocity in m/s; g is the gravity acceleration; $AR = W/H$ is the aspect ratio; W is the tunnel width in m; HRR^* is the non-dimensional heat release rate; ρ_a and c_p are the density in kg/m³ and specific heat in J/(kg · K) of ambient air, respectively.

Table 4. Comparison among sidewall extraction system, longitudinal ventilation system, and the idea ceiling extraction system (no “plug-holing”) with the same air supply rate (61 m³/s).

Test No.	HRR (MW)	Smoke layer length, L_{sm} (m)		Heat removal rate, \dot{Q}_{sm} (MW)	Heat removal efficiency, η (%)	
		Sidewall vent	Longitudinal vent		Sidewall vent	Ideal ceiling vent
1	1.2		99	0.36	30	94
2	1.4		107	0.32	23	85
3	3.3		148	0.84	26	67
4	3.3	>110	154	1.19	36	59
5	3.3		154	0.66	20	51
6	4.8		174	1.01	21	74
7	5.5		181	0.88	16	48
8	6.6		191	1.78	27	59

For the 2 m² pool fire, the smoke can be restricted to about 90 m by using a conventional longitudinal ventilation system. However, with the current sidewall ventilation system, the smoke is observed to flow out from both sides of the portal under all test conditions. In other words, the actual spread distance was more than 110 m, i.e., the distance between the fire source to the rare portal. Furthermore, it can be obtained that the smoke will continue to travel, if the tunnel is longer without an extra extraction vent. However, for the longitudinal ventilation system, the smoke temperature keeps decay during traveling, so does the buoyancy force, where the smoke will be captured by the ventilation airflow finally. Therefore, it is reasonable to suspect that the longitudinal ventilation system may have a better smoke control performance than the sidewall extraction system under the same ventilation

capacity. However, for a long underwater tunnel like the Hong Kong–Zhuhai–Macau Bridge tunnel, it is not possible to use longitudinal ventilation system (Betta *et al.* 2009; Chai *et al.* 2018).

Meanwhile, by comparing the test results with data in (Jiang *et al.* 2018) (the data for the scaled model has been transferred to corresponding full-scale level based on Froude similarity law), it can be found the smoke backlayering length can be controlled in 86 m for the 1.2 MW fire with the same air extraction rate. While for the sidewall extraction system in the current test, the smoke spread distance is much larger (> 110 m). The comparison indicates that the ceiling extraction has a better performance than sidewall smoke extraction system.

During the test, the smoke kept a good stratification state, as shown in Fig. 9. Fresh air was observed to be entrained into the vent in the test, which was similar to the plug-hole effect in tunnel fire scenarios with a vertical shaft. The fresh airflow works as a protection layer, which prevents the smoke layer from settling down and affecting people evacuation. Considering that the smoke spread velocity is around 1 m/s (Fig. 8), which is much lower than the moving speed of human beings at a general level (Seike *et al.* 2017; Fridolf *et al.* 2019). Thus, people in all tested tunnel fire scenarios will have a high possibility to escape from the tunnel.

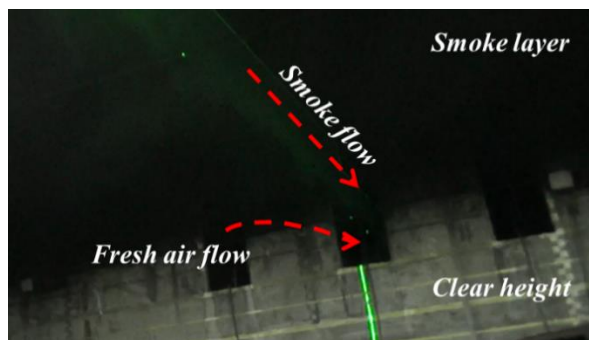


Fig. 9. Fresh airflow and smoke flow extracted into the vent group 5 (60 m fire downstream) in Test No. 7.

Nevertheless, if a longitudinal ventilation system was installed, the ventilation airflow will accelerate the downstream smoke spread velocity. Also, the high-speed airflow will induce a strong shear force at the interface between the smoke layer and fresh air, which would break the smoke stratification and reduce the clear height (Zeng *et al.* 2018). Therefore, compared to the longitudinal ventilation system, the sidewall extraction system has a weaker smoke control ability, but it may be better for people evacuation and safer.

4.2. Heat removal rate and efficiency

Another two important criteria to evaluate the smoke control performance for a transverse ventilation system are the heat removal rate (\dot{Q}_{sm}) and the heat removal efficiency (η). Here, \dot{Q}_{sm} is defined as the additional heat carried by the extracted smoke, as

$$\dot{Q}_{sm} = \int_0^{2m} c_{p,sm} \Delta T(z) u_v dz \quad (9)$$

The heat removal efficiency (η) is defined as the ratio of \dot{Q}_{sm} to the HRR of the fire source, as

$$\eta = \frac{\dot{Q}_{sm}}{HRR} \quad (10)$$

where $c_{p,sm}$ is the specific heat capacity of the smoke; $\Delta T(z)$ is the vertical temperature rise profile measured by the thermocouple lines installed in the vent; u is the airflow velocity of the vent, which was estimated as 7.6 m/s for opening one vent group and 3.8 m/s for opening two vent groups, as described in Section 2. Heat removal rate can better reflect the working efficiency of smoke extraction system than smoke volume removal rate in some respects. For instance, the heat removal rate increases as the fire source gets closer to the vent under the same extraction flow rate. It is because the smoke extracted from the vents was hotter and more dangerous. In short, using the heat removal rate can identify which portion of smoke is more important.

The calculated heat removal rate and heat removal efficiency (η) of the sidewall extraction system are listed in Table 4. The heat removal efficiency varies with HRR: it increases from 30% to 36% when HRR increases from 1.2 MW to 3.3 MW, then decreases to 16% for 5.5 MW fire. The smoke layer is relatively thin for a small fire, and most of the extracted gas is assumed to be cold air. Thus, for a small fire (< 3 MW), increasing the fire HRR, the smoke layer thickness will increase, so more smoke and less fresh air will be extracted; thus, both the rate and efficiency of heat removal will increase. Further increasing the fire HRR (>3 MW), the smoke layer will be thick enough to cover the sidewall vents so that little fresh air will be extracted. Thus, further increasing the fire HRR, the additional smoke cannot be extracted, causing the heat removal efficiency to decrease.

For reference, the maximum heat removal efficiency for an ideal ceiling ventilation system (no “plug-holing”) with the same ventilation capability, geometry, and temperature profile is also calculated and compared in Table 4, where the calculation method referred to (Zhong *et al.* 2021). As expected, the actual heat removal efficiency of the sidewall extraction is clearly lower than the ideal non-plug-holing vent system. In other words, there is a similar plug-holing phenomenon in the sidewall extraction, as visually observed in Fig. 9. Unlike the ceiling vent, some fresh air will always entrain the sidewall vent, if the smoke layer height is higher than the bottom of the vents (e.g., with small HRR or in the early stage of fire). From this perspective, the sidewall smoke extraction used in the underwater tunnel cannot achieve the same heat removal efficiency as the ceiling smoke extraction under the same mechanical ventilation capacity.

4.3. A framework of tunnel-fire database and smart firefighting

With the emerging Artificial Intelligence (AI) technology, the concept of a smart firefighting system attracts more attention (Wu, Park, *et al.* 2021). The state-of-the-art neural networks acquire an organized database to train the AI model to provide an accurate and effective prediction (Wu, Zhang, *et al.* 2021; Zhang, Wu, *et al.* 2021). Full-scale tunnel fire test data are of great significance as they are

close to the actual fire events. In contrast, the advantage of the scaled model and numerical method is low cost for both money and time, which is more suitable for building a database (Zhang et al., 2021). However, the results from scaled and numerical models are inevitably affected by scale effect and simplifying assumptions (Van Maele and Merci 2008; Takeuchi et al. 2018; Tanaka et al. 2018), so the accuracy of these modeled data is always questionable.

The prediction accuracy of the AI model relies heavily on the quality of the database (Ribeiro et al. 2016). Thus, the data generated by scale models and numerical methods, which are not verified by the full-scale data, may cause systematical errors during the training of the AI model (Su et al. 2021; Wu, Park, et al. 2021). The importance of the full-scale data was also highlighted to validate the small-scale model tests and numerical simulations to obtain more reliable data of different fire scenarios. Meanwhile, quantitative analysis of the error induced by the scale effect and simplifying assumptions can only be revealed by the comparison between the AI model prediction and these full-scale test data. Therefore, a solid full-scale database is a foundation to apply the AI-based smart firefighting system.

Moreover, one major problem for the current fire research is the lack of temporal data, and most of the studies only focus on the steady-state fire and smoke behaviors, as reviewed previously (Zhang et al., 2021). It is because the large amount of fire test data varying with time are more difficult to analyze than the spatial data. There is a lack of empirical correlation to explain the time evolution of fire, and most of the non-steady-state data are ignored without further analysis. However, without the time-evolution information of tunnel fire and smoke in the database, the trained AI model cannot make a real-time forecast of the tunnel-fire evolution. Thus, establishing a database of fire tests, including the complete (both raw and processed) temporal data, is needed.

The flow path and prospective of building and using a full-scale test-based database in smart firefighting is illustrated in Fig. 10. To maximize the data usage, the information collected for the full-scale tests should include tunnel geometry and test information, fire information, sensor information, spatial-temporal sensor data, image, and video footprints. Those data can then be applied to train the AI model to predict critical events (smoke back-layering, fire spread, etc.), evacuate fire risks, realize real-time forecast of fire and smoke evolution.

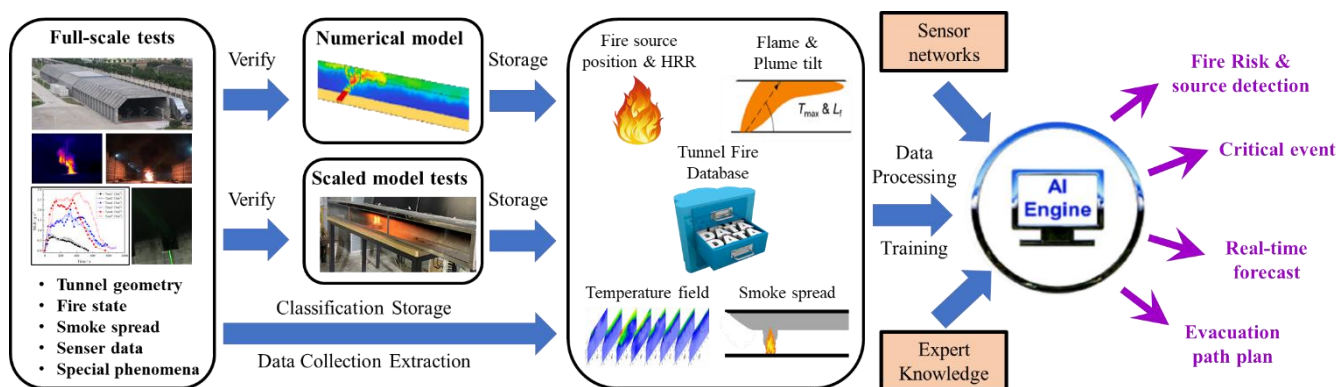


Fig. 10. A framework of full-scale tunnel fire database and AI application in smart firefighting.

The AI-based fire prediction and forecast system was demonstrated with the numerical tunnel fire database in our previous work (Wu, Park, *et al.* 2021; Wu, Zhang, *et al.* 2021; Zhang, Wu, *et al.* 2021) and recently with the temperature sensor network in the reduced-scale tunnel (Wu *et al.* 2022). However, compared with numerical research and reduced-scale experiments, it is quite difficult to conduct these costly large-scale tunnel fire tests, which means that even we construct a database to contain all these data, the majority of the database should be numerical and reduced-scale data. To deal with the imbalance of the reduce-scale model test data and full-scale ones, applying GAN network and transfer learning method to deal with the database of multi-scale tests may be a feasible way and will be investigated in our future work.

Moreover, the imperfection and wrong data due to the unnormal measurement, missing or sensor damage should also be contained in the database. Those imperfection data are also valuable for the training of an attention-based model to identify the weight for different sensors (Vaswani *et al.* 2017), as the sensors in real fire scenarios may also be damaged and cause unnormal data. For instance, although the temperature data of T1 and T6 were not discussed in Fig. 7 due to sensor failure, they are still contained in the database for potential usage in future work.

5. Conclusions

Eight full-scale tunnel fire tests with a sidewall smoke extraction system were carried out with a 1:1 scale (cross-section) of the Hong Kong-Zhu Hai-Macau Bridge tunnel. The effect of sidewall vent and pool size on HRR, smoke temperature distribution, smoke spread, smoke stratification was investigated and analyzed. Major conclusions were summarized as follows:

- (1) The HRR is mainly determined by the pool size. The far-field vent groups have little influence of the HRR. The correlation between HRR and pool-fire area can be fitted by a linear function of $HRR = 1.24 A_F - 0.87 MW$.
- (2) The fire plume tilts to the sidewall vent due to the extraction effect and causes the non-uniform transverse temperature distribution. The non-uniform level decreases as the distance to the fire source increases. The longitudinal temperature decay approximately obeys the exponential law. The decay factor increases with the increase of the HRR and increases when distributing the ventilation capability into two vent groups. A sharp decrease can be observed near the vent region due to the sidewall extraction effect.
- (3) The smoke spread velocity in the current tests varies from 0.8 – 1.2 m/s, lower than people's escape speed. Also, the sidewall jet process is broken by the vent extraction, results in a larger clear-height and better smoke stratification than a longitudinally ventilated tunnel, which could be safer for evacuation.
- (4) The importance of full-scale test data for smart firefighting was highlighted, and a framework and perspective of using the full-scale test-based database in smart firefighting are proposed.

Acknowledgments

This research is funded by the National Key R&D Program of China under Grant No. 2016YFC0800603 and 2016YFC0800604, the Sichuan Provincial Research Program under Grant No. 2016JY0144 and 2021YFS0303, the Fire Bureau of the Ministry of Public Security under Grant No. 2014XFCX16, the Scientific Research Foundation for the Returned Overseas Chinese Scholars from the Ministry of Education, and the Hong Kong Research Grants Council Theme-based Research Scheme (T22-505/19-N). The authors are very grateful to Dr. Dong Yang from Chongqing University for valuable suggestions on designing the tests. TZ thanks the support of Hong Kong PhD Fellowship Scheme.

CRedit author statement

Yaqiang Jiang: Conceptualization, Methodology, Formal analysis, Investigation, Writing - Original Draft, Funding acquisition. **Tianhang Zhang:** Methodology, Formal analysis, Investigation, Writing - Original Draft. **Shuai Liu:** Investigation, Resources. **Qinli He:** Investigation, Resources. **Le Li:** Investigation, Resources. **Xinyan Huang:** Formal analysis, Supervision; Writing-Review & Editing, Funding acquisition.

References

- Beard A, Carvel R (2012) 'Handbook of tunnel fire safety.' (ICE Publishing)
- Betta V, Cascetta F, Musto M, Rotondo G (2009) Numerical study of the optimization of the pitch angle of an alternative jet fan in a longitudinal tunnel ventilation system. *Tunnelling and Underground Space Technology* **24**, 164–172. doi:10.1016/j.tust.2008.06.002.
- Chai L, Wang X, Han X, Song J, Lei P, Xia Y, Wang Y (2018) Complementary ventilation design method for a highway twin-tunnel based on the compensation concept. *Mathematical Problems in Engineering* **2018**,. doi:10.1155/2018/2393272.
- Chen LF, Hu LH, Tang W, Yi L (2013) Studies on buoyancy driven two-directional smoke flow layering length with combination of point extraction and longitudinal ventilation in tunnel fires. *Fire Safety Journal* **59**, 94–101. doi:10.1016/j.firesaf.2013.04.003.
- Delichatsios MA (1981) The flow of fire gases under a beamed ceiling. *Combustion and Flame* **43**, 1–10. doi:10.1016/0010-2180(81)90002-X.
- Drysdale D (2011) 'An Introduction to Fire Dynamics.' (John Wiley & Sons, Ltd: Chichester, UK) doi:10.1002/9781119975465.
- Fridolf K, Ronchi E, Nilsson D, Frantzich H (2019) The representation of evacuation movement in smoke-filled underground transportation systems. *Tunnelling and Underground Space Technology* **90**, 28–41. doi:10.1016/j.tust.2019.04.016.
- Fu EY, Tam WC, Wang J, Peacock R, Reneke PA, Ngai G, Leong HV, Cleary T (2021) Predicting Flashover Occurrence using Surrogate Temperature Data. In 'The Thirty-Fifth AAAI Conference on Artificial Intelligence (AAAI-21)',
- Hu LH, Huo R, Chow WK (2008) Studies on buoyancy-driven back-layering flow in tunnel fires. *Experimental Thermal and Fluid Science*. doi:10.1016/j.expthermflusci.2008.03.005.
- Hu LH, Huo R, Peng W, Chow WK, Yang RX (2006) On the maximum smoke temperature under the

- ceiling in tunnel fires. *Tunnelling and Underground Space Technology* **21**, 650–655. doi:10.1016/j.tust.2005.10.003.
- Hu LH, Huo R, Wang HB, Li YZ, Yang RX (2007) Experimental studies on fire-induced buoyant smoke temperature distribution along tunnel ceiling. *Building and Environment* **42**, 3905–3915. doi:10.1016/j.buildenv.2006.10.052.
- Hu LH, Huo R, Wang HB, Yang RX (2007) Experimental and numerical studies on longitudinal smoke temperature distribution upstream and downstream from the fire in a road tunnel. *Journal of Fire Sciences* **25**, 23–43. doi:10.1177/0734904107062357.
- Hu L, Li YZ, Huo R, Yi L, Chow WK (2006) Full-scale experimental studies on mechanical smoke exhaust efficiency in an underground corridor. *Building and Environment* **41**, 1622–1630. doi:10.1016/j.buildenv.2005.06.025.
- Hu LH, Peng W, Yang RX (2014) Fundamentals of tunnel fire dynamics and prevention technology.
- Hu LH, Tang W, Chen LF, Yi L (2013) A non-dimensional global correlation of maximum gas temperature beneath ceiling with different blockage–fire distance in a longitudinal ventilated tunnel. *Applied Thermal Engineering* **56**, 77–82. doi:10.1016/j.applthermaleng.2013.03.021.
- Ingason H, Li Y (2011) Model scale tunnel fire tests with point extraction ventilation. *Journal of Fire Protection Engineering* **21**, 5–36. doi:10.1177/1042391510394242.
- Ingason H, Li YZ, Lönnemark A (2015) Runehammar tunnel fire tests. *Fire Safety Journal* **71**, 134–149. doi:10.1016/j.firesaf.2014.11.015.
- Ingason H, Li YZ, Lönnemark A, Lonnermakr A (2015) ‘Tunnel fire dynamics.’ (Springer: London) doi:10.1007/978-1-4939-2199-7.
- Ingason H, Lönnemark A (2005) Heat release rates from heavy goods vehicle trailer fires in tunnels. *Fire Safety Journal* **40**, 646–668. doi:10.1016/j.firesaf.2005.06.002.
- Ji J, Bi Y, Venkatasubbaiah K, Li K (2016) Influence of aspect ratio of tunnel on smoke temperature distribution under ceiling in near field of fire source. *Applied Thermal Engineering* **106**, 1094–1102. doi:10.1016/j.applthermaleng.2016.06.086.
- Ji J, Gao ZH, Fan CG, Zhong W, Sun JH (2012) A study of the effect of plug-holing and boundary layer separation on natural ventilation with vertical shaft in urban road tunnel fires. *International Journal of Heat and Mass Transfer* **55**, 6032–6041. doi:10.1016/j.ijheatmasstransfer.2012.06.014.
- Jiang L, Ingason H (2020) Use of mobile fans during tunnel fires. *Tunnelling and Underground Space Technology* **106**, 103618. doi:10.1016/j.tust.2020.103618.
- Jiang X, Liu M, Wang J, Li Y (2018) Study on induced airflow velocity of point smoke extraction in road tunnel fires. *Tunnelling and Underground Space Technology* **71**, 637–643. doi:10.1016/j.tust.2017.09.020.
- Kunsch JP (2002) Simple model for control of fire gases in a ventilated tunnel. *Fire Safety Journal* **37**, 67–81.
- Kurioka H, Oka Y, Satoh H, Sugawa O (2003) Fire properties in near field of square fire source with longitudinal ventilation in tunnels. *Fire Safety Journal* **38**, 319–340. doi:10.1016/S0379-7112(02)00089-9.
- Lee EJ, Oh CB, Oh KC, Yoo YH, Shin HJ (2010) Performance of the smoke extraction system for fires in the Busan-Geoje immersed tunnel. *Tunnelling and Underground Space Technology* **25**, 600–606. doi:10.1016/j.tust.2010.04.005.
- Li YZ, Ingason H (2017) Effect of cross section on critical velocity in longitudinally ventilated tunnel fires. *Fire Safety Journal* **91**, 303–311. doi:10.1016/j.firesaf.2017.03.069.
- Li ZY, Lei B, Ingason H (2010) Study of critical velocity and backlayering length in longitudinally

- ventilated tunnel fires. *Fire Safety Journal* **45**, 361–370. doi:10.1016/j.firesaf.2010.07.003.
- Lin CJ, Chuah YK (2008) A study on long tunnel smoke extraction strategies by numerical simulation. *Tunnelling and Underground Space Technology* **23**, 522–530. doi:10.1016/j.tust.2007.09.003.
- Liu S, Jiang YQ, Chen JZ, Li K (2016) Full-scale Experimental Research on the effect of Smoke Exhaust Strategies on Efficiency of Point Extraction System in an Underwater Tunnel. *Procedia Engineering* **166**, 362–372. doi:10.1016/j.proeng.2016.11.561.
- Liu B, Mao J, Xi Y, Hu J (2021) Effects of altitude on smoke movement velocity and longitudinal temperature distribution in tunnel fires. *Tunnelling and Underground Space Technology* **109**, 103784. doi:10.1016/j.tust.2021.103850.
- Lönnermark A, Persson B, Ingason H (2006) Pulsations during large-scale fire tests in the Runehamar tunnel. *Fire Safety Journal* **41**, 377–389. doi:10.1016/j.firesaf.2006.02.004.
- Van Maele K, Merci B (2008) Application of RANS and LES field simulations to predict the critical ventilation velocity in longitudinally ventilated horizontal tunnels. *Fire Safety Journal* **43**, 598–609. doi:10.1016/j.firesaf.2008.02.002.
- Ribeiro MT, Singh S, Guestrin C (2016) ‘Why should i trust you?’ Explaining the predictions of any classifier. In ‘Proceedings of the ACM SIGKDD International Conference on Knowledge Discovery and Data Mining’, 1135–1144 doi:10.1145/2939672.2939778.
- Seike M, Kawabata N, Hasegawa M (2017) Evacuation speed in full-scale darkened tunnel filled with smoke. *Fire Safety Journal* **91**, 901–907. doi:10.1016/j.firesaf.2017.04.034.
- Su L chu, Wu X, Zhang X, Huang X (2021) Smart performance-based design for building fire safety: Prediction of smoke motion via AI. *Journal of Building Engineering* **43**, 102529. doi:10.1016/j.job.2021.102529.
- Takeuchi S, Tanaka F, Yoshida K, Moinuddin KAM (2018) Effects of scale ratio and aspect ratio in predicting the longitudinal smoke- temperature distribution during a fire in a road tunnel with vertical shafts. *Tunnelling and Underground Space Technology* **80**, 78–91. doi:10.1016/j.tust.2018.05.020.
- Tanaka F, Takezawa K, Hashimoto Y, Moinuddin KAM (2018) Critical velocity and backlayering distance in tunnel fires with longitudinal ventilation taking thermal properties of wall materials into consideration. *Tunnelling and Underground Space Technology* **75**, 36–42. doi:10.1016/j.tust.2017.12.020.
- Vaswani A, Shazeer N, Parmar N, Uszkoreit J, Jones L, Gomez AN, Kaiser L, Polosukhin I (2017) Attention is all you need. *arXiv preprint arXiv:1706.03762*.
- Vauquelin O, Mégret O (2002) Smoke extraction experiments in case of fire in a tunnel. *Fire Safety Journal* **37**, 525–533. doi:10.1016/S0379-7112(02)00014-0.
- Wu Y, Bakar MZA (2000) Control of smoke flow in tunnel fires using longitudinal ventilation systems - a study of the critical velocity. *Fire Safety Journal*. doi:10.1016/S0379-7112(00)00031-X.
- Wu X, Park Y, Li A, Huang X, Xiao F, Usmani A (2021) Smart Detection of Fire Source in Tunnel Based on the Numerical Database and Artificial Intelligence. *Fire Technology* **57**, 657–682. doi:10.1007/s10694-020-00985-z.
- Wu X, Zhang X, Huang X, Xiao F, Usmani A (2021) A real-time forecast of tunnel fire based on numerical database and artificial intelligence. *Building Simulation*. doi:10.1007/s12273-021-0775-x.
- Wu X, Zhang X, Jiang Y, Huang X, Huang GGQ, Usmani A (2022) Intelligent tunnel fire safety monitoring system : Framework and small-scale demonstration. *Tunnelling and Underground*

- Space Technology* 104301. doi:10.1016/j.tust.2021.104301.
- Xu P, Jiang SP, Xing RJ, Tan JQ (2018) Full-scale immersed tunnel fire experimental research on smoke flow patterns. *Tunnelling and Underground Space Technology* **81**, 494–505. doi:10.1016/j.tust.2018.08.009.
- Xu P, Xing RJ, Jiang SP, Li LJ (2019) Theoretical prediction model and full-scale experimental study of central smoke extraction with a uniform smoke rate in a tunnel fire. *Tunnelling and Underground Space Technology* **86**, 63–74. doi:10.1016/j.tust.2019.01.014.
- Xu QQ, Yi L, Xu ZS, Wu DX (2013) Preliminary study on exhaust efficiency of smoke management system in tunnel fires. *Procedia Engineering* **52**, 514–519. doi:10.1016/j.proeng.2013.02.177.
- Yan Z guo, Guo Q hua, Zhu H hua (2017) Full-scale experiments on fire characteristics of road tunnel at high altitude. *Tunnelling and Underground Space Technology* **66**, 134–146. doi:10.1016/j.tust.2017.04.007.
- Yang D, Hu LH, Huo R, Jiang YQ, Liu S, Tang F (2010) Experimental study on buoyant flow stratification induced by a fire in a horizontal channel. *Applied Thermal Engineering* **30**, 872–878. doi:10.1016/j.applthermaleng.2009.12.019.
- Yang Y, Liu C, Long Z, Qiu P, Chen J, Zhong M (2020) Full-scale experimental study on fire under vehicle operations in a sloped tunnel. *International Journal of Thermal Sciences* **158**, 106524. doi:10.1016/j.ijthermalsci.2020.106524.
- Yi L, Wei R, Peng J, Ni T, Xu Z, Wu D (2015) Experimental study on heat exhaust coefficient of transversal smoke extraction system in tunnel under fire. *Tunnelling and Underground Space Technology* **49**, 268–278. doi:10.1016/j.tust.2015.05.002.
- Zabetakis MG, Burgess DS (1961) ‘Research on the hazards associated with the production and handling of liquid hydrogen.’ (US Department of the Interior, Bureau of Mines)
- Zeng Z, Xiong K, Lu XL, Weng MC, Liu F (2018) Study on the smoke stratification length under longitudinal ventilation in tunnel fires. *International Journal of Thermal Sciences* **132**, 285–295. doi:10.1016/j.ijthermalsci.2018.05.038.
- Zhang T, Wang G, Hu H, Huang Y, Zhu K, Wu K (2021) Study on temperature decay characteristics of fire smoke backflow layer in tunnels with wide-shallow cross-section. *Tunnelling and Underground Space Technology* **112**,. doi:10.1016/j.tust.2021.103874.
- Zhang X, Wu X, Park Y, Zhang T, Huang X, Xiao F, Usmani A (2021) Perspectives of big experimental database and artificial intelligence in tunnel fire research. *Tunnelling and Underground Space Technology* **108**, 103691. doi:10.1016/j.tust.2020.103691.
- Zhao S, Liu F, Wang F, Weng M (2018) Experimental studies on fire-induced temperature distribution below ceiling in a longitudinal ventilated metro tunnel. *Tunnelling and Underground Space Technology* **72**, 281–293. doi:10.1016/j.tust.2017.11.032.
- Zhong W, Sun C, Bian H, Gao Z, Zhao J (2021) The plug-holing of lateral mechanical exhaust in subway station: Phenomena, analysis, and numerical verification. *Tunnelling and Underground Space Technology* **112**, 103914. doi:10.1016/j.tust.2021.103914.